Thermal Science and Engineering Progress, Volume 20, December 2020, Article number 100723
DOI:10.1016/j.tsep.2020.100723

Supercritical CO_2 cycle for coal-fired power plant based on calcium looping combustion

Dawid P. Hanak, Sebastian Michalski, Vasilije Manovic*

Energy and Power, School of Water, Energy and Environment, Cranfield University,

Bedford, Bedfordshire, MK43 0AL, UK

Corresponding author: *Dawid P. Hanak, d.p.hanak@cranfield.ac.uk

Abstract

Calcium looping combustion (CaLC), which comprises an indirectly-heated calciner, is characterised with lower energy intensity and economic penalties compared to that of mature CO_2 capture technologies. As CaLC is a standalone power boiler, integration of advanced power cycles can lead to further improvement in net efficiency and reduction in the cost of electricity. Therefore, this study aimed to propose routes for the integration of the supercritical CO_2 cycle (sCO_2) with CaLC and to evaluate their benefits with respect to the conventional steam cycle. Such processes were modelled in Aspen Plus™. Moreover, the effect of the operating conditions on the techno-economic performance of the considered cases was evaluated. This study has shown that implementation of the optimised recompression sCO_2 cycle with a clean gas cooler resulted in the net efficiency and break-even price of electricity of 37.3%$_{HHV}$ and 75.13 €/MWh, respectively. These are 0.7%$_{HHV}$ points lower and 26% higher, respectively, than that of the conventional coal-fired power plant without CO_2 capture. Such performance, however, is superior to retrofits of coal-fired power plants with mature CO_2 capture technologies as well as CaLC with a conventional steam cycle, proving the benefits of linking CaLC with advanced power cycles.

Key Words: heat recovery; advanced power cycles; CO_2 capture; techno-economic analysis; solid looping cycles; carbonate looping

1 Introduction

The Intergovernmental Panel on Climate Change [1] reported that if the current rate of the global mean temperature increase persists, it is highly probable that it will exceed the pre-industrial level by more than 1.5°C between 2030–2050. Such an increase is associated with global warming caused by greenhouse gas (GHG) emissions, primarily CO_2. Combustion of coal for heat and electricity production was associated with 44.1% of global CO_2 emission in 2016 [2]. Currently, the electricity production in coal-fired power plants meets about 38% of global electricity demand [2], and is responsible for 30% of global CO_2 emissions [3]. Such a high global share of coal is driven primarily by the investments in China and India [4]. Importantly, a significant fraction of the current coal-fired power plant capacity (~75%) [5] is based on inefficient subcritical units that operate with main steam pressure and temperature below 221 bar and 565°C, respectively, and achieve net efficiencies of about 33% [6]. Therefore, the power sector is a significant contributor to global CO_2 emissions [7]. As a result, all the scenarios investigated by van Vuuren et al. [8] reflected a significant deployment of carbon capture and storage (CCS) for decarbonisation of coal-fired power plants, especially in the projected primary energy mix at the start of the next century.

Amine scrubbing is currently considered as the mature technology for CO_2 capture, with the technology readiness level (TRL) of 9 [9]. According to Mantripragada et al. [10], integrating this technology in a supercritical coal-fired power plant in a similar way as in Boundary Dam would cause a net efficiency penalty of 10.2% points. A continuous development of amine scrubbing, which focuses on the development of new process-intensified equipment [11] or more efficient solvents [12,13], and of emerging CO_2 capture technologies, such as calcium looping (CaL) [14], which is currently at TRL 6 [9], has significantly decreased the efficiency penalties and CO_2 avoided costs.

CaL is considered as an emerging technology that has been demonstrated experimentally at a scale below 2 MW_{th} [15,16]. Its performance has been mainly evaluated at the process level using thermodynamic and process models, and at the reactor level using the computational fluid dynamic models. This is because the use of process simulation and modelling tools enables cost-effective design, assessment

and optimisation of CO_2 capture technologies, such as CaL, and of their integration with power plants [17]. Two main approaches have been used to assess the integration of CaL with power plants. The first approach relies on soft-linking of CaL and power plant models, which are developed in separate software and converged in an iterative process. Berstad et al. [18] assessed retrofit of CaL to a natural gas combined cycle (NGCC) power plant, the latter of which was modelled in Aspen Hysys®. The performance of CaL was characterised using a thermodynamic model, which considered heat and mass balances, developed in MS Excel. This model also used a semi-empirical correlation for sorbent deactivation derived by Rodríguez et al. [19] to estimate the average sorbent conversion in the carbonator. This work indicated that retrofit of CaL to NGCC will result in the net efficiency penalty of 6.8–8.4%$_{LHV}$. Cormos [20] assessed retrofit of CaL to a coal-fired power plant (CFPP), the latter of which was modelled in Thermoflex®. The performance of CaL was estimated using a process model developed in ChemCAD®. This model assumed that the carbonator and calciner operate under chemical equilibrium conditions that were determined using the Gibbs free energy minimisation approach. This work revealed that CaL retrofit to subcritical CFPP, supercritical CFPP and integrated gasification combined cycle power plant will result in the net efficiency penalty of 5.3%$_{LHV}$, 7.4%$_{LHV}$, and 10.1%$_{LHV}$, respectively. Moreover, the cost of CO_2 avoided was estimated to be 28.2 €/tCO_2, 31.3 €/tCO_2 and 31 €/tCO_2, respectively. The second approach relies on hard-linking of CaL and power plant models, which are developed in a common simulation environment. Hanak et al. [21,22] developed the process model of integrated supercritical CFPP and CaL in Aspen Plus®. This model used the same approach to characterise sorbent performance as the study by Berstad et al. [18]. This study showed that CaL retrofit to a supercritical CFPP will result in the net efficiency penalty of 7.9%$_{HHV}$ and the cost of CO_2 avoided of 41.6–57.3 €/tCO_2. Erans et al. [23] developed the process model for NGCC and integrated it with the process model for CaL developed by Hanak et al. [21] in Aspen Plus®. This work revealed that retrofit of CaL to NGCC will lead to the net efficiency penalty of 8.6–12%$_{LHV}$ and the cost of CO_2 avoided of 29.3 €/tCO_2. Rolfe et al. [24,25] developed the process model for the integrated supercritical CFPP and CaL in the in-house ECLIPSE Process Simulator [26]. Their work estimated that the cost of CO_2 avoided for CaL is 20–22.3 €/tCO_2, at net efficiency penalty of 7–7.4%$_{LHV}$ points.

It is important to emphasise that in CaL the net efficiency penalty is primarily caused by the energy requirement in the air separation unit (ASU) that provides high-purity O_2 for sorbent regeneration in the calciner under oxy-combustion conditions. To alleviate the need for the energy-intensive ASU, Hanak and Manovic [27] considered an indirectly heated calciner in the standalone technology called calcium looping combustion (CaLC). This process, which was modelled in Aspen Plus®, uses an external coal-fired combustion chamber to provide heat to sustain the calcination reaction. The CaLC-based power plant without the CO_2 compression train (CCT) was shown to have a net efficiency comparable to that of conventional coal-fired power plants and to produce high-purity CO_2. Considering the energy requirement of CCT, a net efficiency of the CaLC-based power plant was 2.4%$_{HHV}$ points below that of a conventional power plant.

Improvement of the techno-economic performance of both conventional and CaLC-based power plants can be achieved by the implementation of advanced closed Brayton cycles (CBCs) that have currently been developed for solar and nuclear power plants [28–30]. This is because the CBCs, with working media such as CO_2, He or Xe, are characterised by relatively low investment costs and similar, or even higher, thermal efficiencies compared to supercritical and ultra-supercritical steam cycles [31]. The work by Michalski et al. [32], which was performed in Aspen Plus®, has proven that the sCO_2 cycle resulted in the best techno-economic performance of the CaLC-based power plant among considered working media in CBC (CO_2, He, Xe, N_2). The study by Dostal et al. [33], which represented power cycles using FORTRAN, has confirmed that the capital cost of the sCO_2 cycle is 24% lower than that of the steam cycle. Le Moullec [34] has demonstrated that a coal-fired power plant with a sCO_2 cycle, which was modelled in Aspen Plus®, can achieve a net efficiency of 50.3%$_{LHV}$ at the turbine inlet temperature of 620°C and the compressor outlet pressure of 300 bar. This was shown to be 4.8% points higher than the net efficiency of the corresponding coal-fired power plant with the conventional steam cycle (45.5%). As a result, the retrofit of amine scrubbing to the coal-power plant with the sCO_2 cycle resulted in the efficiency penalty of only 1% point with the increase in the levelised cost of electricity of 22%. Furthermore, Hanak and Manovic [35] has shown that the replacement of the conventional steam cycle with the recompression sCO_2 cycle, which was modelled in Aspen Plus®, can reduce the efficiency penalty of CaL from

7.9%$_{HHV}$ points to 5.8%$_{HHV}$ points. Wei et al. [36] has shown that use of the simple sCO_2 cycle in place of the conventional steam cycle in the oxy-combustion coal-fired power plant, which was modelled in Aspen Plus®, can reduce the efficiency penalty from 10.3%$_{HHV}$ points to 8.3%$_{HHV}$ points, and reduce the levelised cost of electricity by up to 4%. In this vein, Marchionni et al. [28] has considered different layouts of the sCO_2 cycle using CycleTempo. Their study demonstrated that the capital cost of the simple sCO_2 cycle is 26.6% lower than that for the recompression sCO_2. However, its net efficiency is approximately 1.5% points lower than that for the recompression sCO_2 cycle.

Deployment of novel low-CO_2-emission combustion systems integrated with advanced power cycles is expected to contribute toward decarbonisation of the power sector, ensuring a secure supply of energy at an affordable cost. Considering the trade-off between net efficiency and capital cost, the layout of the sCO_2 cycle needs to be selected to maximise the techno-economic performance of the entire system. Although the sCO_2 cycle has been shown to be most efficient among other CBCs for CaLC, the impact of its layout on the techno-economic performance has not been assessed. Therefore, the primary focus of this study is to propose and compare strategies to integrate the sCO_2 cycle with CaLC that maximises the net efficiency and minimises the break-even price of electricity of the CaLC–based power plant. The capital costs of the considered cases are estimated using a bottom-up approach and economic performance is evaluated using the net present value (NPV) method. Furthermore, the influence of the key thermodynamic parameters on the techno-economic performance is assessed in a parametric study to establish the optimum operating conditions. Finally, the techno-economic performance of the considered CaLC-based power plants with sCO_2 cycle is benchmarked with a CaLC-based power plant with conventional steam cycle and a conventional coal-fired power plant without CO_2 capture.

2 METHODS

2.1 Process description and modelling

The concepts of the CaLC-based power plant developed in this work comprise three main subsystems that were modelled in Aspen Plus®:

- the CaLC for low-carbon thermochemical conversion of chemical energy in the

solid fuel to thermal energy;

- CCT for compression and conditioning of CO_2 prior to its transportation and storage; and
- the power cycle for the conversion of thermal energy to electrical energy.

The CaLC and CCT subsystems were modelled using the Peng-Robinson Mathias-Boston equation of state. The sCO_2 cycle was modelled using the Lee-Kesler-Plöcker equation-of-state to accurately account for nonlinear behaviour of CO_2 under supercritical conditions.

The process model for the CaLC subsystem has been developed by Hanak and Manovic [27], based on the CaL model that was validated with the experimental data from 1.7 MW_{th} la Pereda pilot plant [21,37]. The heat required to sustain the calcination process in CaLC is provided indirectly from an external coal-fired combustor. Both the calciner and the combustor were modelled as Gibbs reactors (*RGibbs*), while the carbonator was modelled as a stoichiometric reactor (*RStoic*). The sorbent circulation rate was determined to achieve the overall CO_2 capture level of 90%. This parameter accounts for CO_2 emissions from both the calcination process and combustion. The average sorbent conversion was estimated using the semi-empirical correlation proposed by Rodríguez et al. [19], and the experimental curve from the la Pereda pilot plant to represent sorbent deactivation [37]. The detailed description of CaLC (Figure 1) was presented by Hanak and Manovic [27]. The concentrated CO_2 stream from CaLC is then processed and conditioned for transport in the CCT subsystem (Figure 1). The CO_2 stream is compressed in a nine-stage intercooled compressor (*MComp*) and a pump (*Pump*). Initial operating conditions of the main subsystems are summarised in Table 1. The cases of the CaLC-based power plant proposed in this study differ in the structures of the sCO_2 cycle. The main heat sources available in CaLC include flue gas from the coal-fired combustor and clean gas from the carbonator, as well as the heat liberated in the exothermal reaction in the carbonator. These are integrated in the considered sCO_2 cycle structures, the detailed description of which is provided in Sections 2.2–2.4.

Table 1: Assumptions for a process model of calcium looping combustion and CO_2 compression train [27,38]

Subsystem	Parameter	Value
Combustor	Coal (Illinois No 6) higher heating value (MJ/kg) [39]	27.01
	Specific power consumption of coal preparation system (MJ/t_{coal})	8.2
	Minimum temperature (°C)	1000
	O_2 concentration in flue gas (%)	3
	Pressure drop (mbar)	150
Calciner	Calcination extent (-)	0.95
	Operating temperature (°C)	900
	Pressure drop (mbar)	150
	Relative make-up (-)	0.03
	Fraction of recycled CO_2 (-)	0.2
	Specific power consumption of sorbent purge system ($MJ/t_{ash/sorbent}$)	31.2
Carbonator	Carbonation extent (-)	0.7
	Operating temperature (°C)	650
	Pressure drop (mbar)	150
	Specific power consumption of sorbent preparation system ($MJ/t_{sorbent}$)	52.4
Heat exchanger network	Minimum temperature approach of air preheater(°C)	10
	Minimum temperature approach of CO_2 preheater (°C)	100
	Cold-end temperature difference of the carbonator clean gas cooler (°C)	20
	Minimum temperature approach of sorbent heat exchangers (°C)	25
CO_2 compression train	Polytropic efficiency of compressor stages (%)	77–80
	Isentropic efficiency of pump(%)	85
	Mechanical efficiency of compressor and pump (%)	99.6
	Compressor/pump outlet pressure (MPa)	7.4/11
	Outlet temperature of intercoolers(°C)	40
	Cold/hot-end temperature difference of intercoolers (°C)	15/30
	Cold/hot-end temperature difference of CO_2 condenser (°C)	5/30
	Overall heat transfer coefficient of intercoolers ($W/m^2°C$)	300

2.1.1 Reference case with a supercritical steam cycle

The CaLC-based power plant with a supercritical steam cycle (Figure 1), which is considered as a reference case in this study, has been described by Hanak and Manovic [27]. It assumes that the high-grade heat available in CaLC is utilised to raise the steam for the supercritical steam cycle that is characterised with the main and reheat steam parameters of 593.3°C/24.2 MPa and 593.3°C/4.9 MPa, respectively. The remaining thermodynamic assumptions for the considered steam cycle are presented in Table 2.

Table 2: Process model assumptions for supercritical steam cycle [27]

Parameter	Value
Feedwater heater terminal temperature difference (°C)	10.0
Feedwater heater minimum temperature approach (°C)	2.8
Isentropic efficiency of a high-pressure steam turbine (%)	83.8–84.5
Isentropic efficiency of a high/intermediate/low-pressure steam turbine (%)	88.0
Isentropic efficiency of a high/intermediate/low-pressure steam turbine (%)	88.0–92.7
Isentropic efficiency of pumps (%)	80.0
Electrical efficiency of a generator (%)	98.5
Mechanical efficiency of steam turbines (%)	99.8

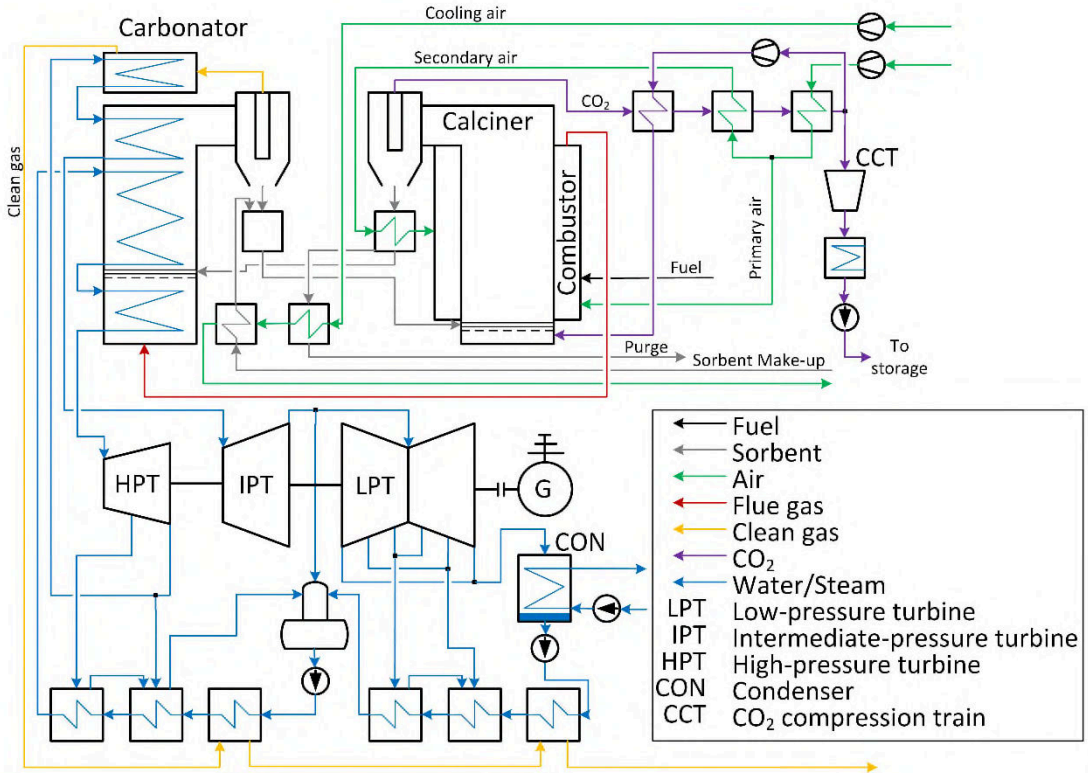

Figure 1: Process flow diagram of calcium looping combustion with a supercritical steam cycle (Reference case)

2.1.2 Simple supercritical CO_2 cycle with clean gas cooler

The CaLC-based power plant with a simple sCO_2 cycle and a clean gas cooler (CGC) is presented in Figure 2 (Case 1). The detailed description of this case is available in Michalski et al. [38]. The thermodynamic model of the sCO_2 cycle was developed by Hanak and Manovic [15]. The accuracy of its prediction was validated with experimental [40] and simulation [34] data. The main advantage of Case 1 is that it maximises the high-grade heat available in the clean gas stream by incorporation of CGC. Thermodynamic assumptions for Case 1 are summarised in Table 3.

Table 3: Initial process model assumptions for supercritical CO_2 cycle and clean gas cooler (Case 1) [38]

Parameter	Value
Compressor isentropic efficiency (%)	85
Compressor inlet/outlet pressure (MPa)	7.4/20
Compressor inlet temperature (°C)	31.3
Expander isentropic efficiency (%)	93
Expander inlet temperature (°C)	600
Compressor/Expander mechanical efficiency (%)	99
Electric generator efficiency (%)	98.5
Carbonator cooler cold side relative pressure loss (%)	0.5
Clean gas cooler cold-end temperature difference (°C)	20
Clean gas cooler cold-side relative pressure loss (%)	0.3
Flue gas cooler cold-side relative pressure loss (%)	0.2
Low-temperature recuperator cold/hot-end temperature difference (°C)	5/5
High-temperature recuperator cold-end temperature difference (°C)	10
Low-temperature and high-temperature recuperator cold-side relative pressure loss (%)	0.5
Low-temperature and high-temperature recuperator hot-side relative pressure loss (%)	1.0
Low-temperature and high-temperature recuperator overall heat transfer coefficient ($W/m^2°C$) [28]	1700
Cooling water temperature at the cooler outlet (°C)	25
Cooler hot-side relative pressure loss (%)	1.0
Cooler overall heat transfer coefficient ($W/m^2°C$) [28]	2900
Water pump pressure ratio (-)	2.0
Cooling water parameters at the inlet to the water pump (°C/MPa)	20/0.1

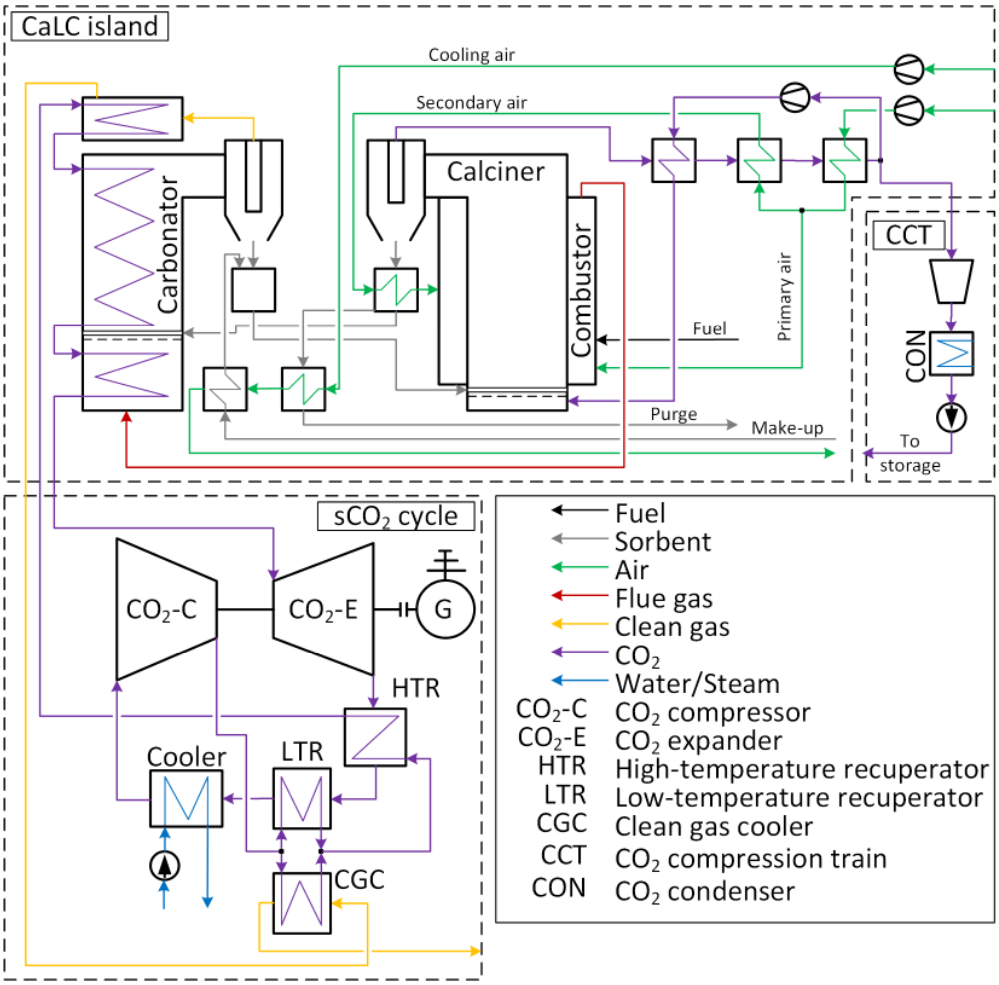

Figure 2. Power plant based on calcium looping combustion with simple supercritical CO_2 cycle and clean gas cooler (Case 1)

2.1.3 Recompression supercritical CO_2 cycle

The structure of a recompression sCO_2 cycle (Case 2) is presented in Figure 3. The main advantage of this structure is that it maximises the thermal efficiency of the sCO_2 cycle. Compared to Case 1, Case 2 includes a recompressor, which has an isentropic efficiency of 85%, and does not include the CGC. The recompressor is fed with the CO_2 stream from the splitter located before the cooler. The compressed stream is then mixed with the CO_2 stream heated in the LTR. It was assumed that the outlet pressure of the recompressor is equal to that of the CO_2 stream leaving the cold side of the LTR. Moreover, the hot-end temperature difference of the LTR was assumed to be 5°C. The remaining assumptions are the same as in Table 2.

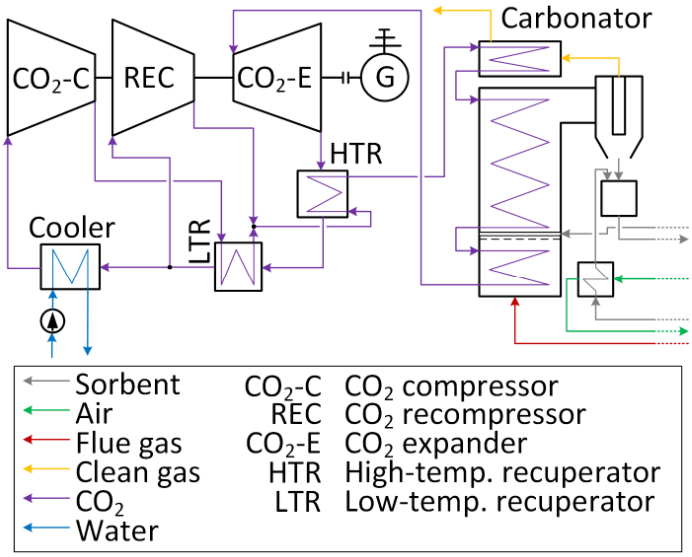

Figure 3: Recompression supercritical CO_2 cycle (Case 2)

2.1.4 Recompression supercritical CO_2 cycle with clean gas cooler

The structure presented in Figure 4 (Case 3) combines the benefits of the structures presented in Case 1 (maximisation of heat utilisation) and Case 2 (maximisation of the thermal efficiency of the sCO_2 cycle). Therefore, this structure comprises both the recompressor and the CGC. As opposed to Case 1, the CO_2 stream heated in the CGC is mixed with the CO_2 stream leaving the HTR. The split ratio, which is defined as the fraction of the CO_2 stream leaving the cooler that is directed to the recompressor, is adjusted to equalise the temperatures of the mixed CO_2 streams. The remaining assumptions are the same as in Table 2.

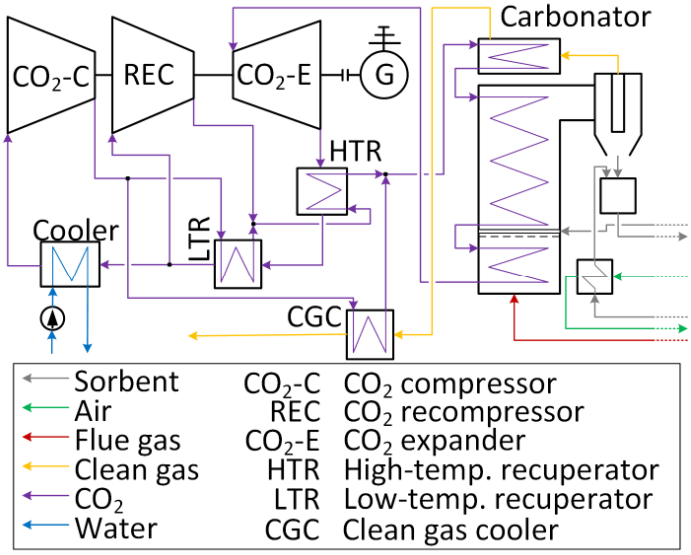

Figure 4: Recompression supercritical CO_2 cycle with clean gas cooler (Case 3)

2.2 Techno-economic feasibility assessment framework

The techno-economic assessment performed in this work utilises the framework that has been proposed by Michalski et al. [38]. The net efficiency of the CaLC-based power plant, which is defined in Eq. (1), is the key performance indicator for thermodynamic feasibility of the considered cases. It depends on the fuel flow rate ($\dot{m}_F$), higher heating value (*HHV*) of fuel, total auxiliary power requirement ($\sum P_{AUX}$) and gross power output (P_G).

$$\eta_N = \frac{P_G - \sum P_{AUX}}{\dot{m}_F \cdot HHV} \tag{1}$$

The break-even price of electricity (BEP_{el}) is the key performance indicator that quantifies the economic feasibility of the CaLC-based power plant. To estimate BEP_{el}, the value of the electricity price is changed iteratively until the NPV reaches zero [41–43]. The NPV (Eq. (2)) depends on the discounted annual cash flows (CF_t), total number of building and operation years (n), the current building/operation year (t), and discount rate (r). A discount rate of 6% was used in this study [44]. Initially, the carbon tax of 0 €/t was assumed. The remaining assumptions used in the economic assessment of the CaLC-based power plants are presented in Table 4.

$$NPV = \sum_{t=1}^{t=n} \frac{CF_t}{(1+r)^t} \tag{2}$$

Table 4: Assumptions for the economic assessment of the calcium looping combustion-based power plant

Parameter	Value
Building period time (years)	4
Exploitation time (years)	25
Capacity factor (%) [39]	85
Corporate tax rate (%)	19
Commercial loan coverage of the total as-spent investment cost (%)	80
Commercial loan interest rate (%).	6
Commercial loan repayment time (years)	15
Depreciation time (years)	10
Fresh sorbent cost (€/t) [39]	29.3
Ash and spent sorbent disposal unit cost (€/t) [39]	22
sCO_2 cycle exploitation cost (€/h) [38]	403.03
Annual average salary of a single employee (k€) [45]	43.9
Employment rate (person/$MW_{el,gross}$) [46]	0.2
Fuel (coal) cost (€/t) [47]	58.75
Repair cost as part of the total investment costs (%) [38]	0.5-2.5
Insurance cost as part of the total investment costs (%) [38]	0.5
Salvage value as part of the total investment costs (%) [38]	20

The total as-spent investment cost (TASC), defined in Eq. (3), is based on the cost estimation results presented in Fout et al. [39]. The TASC relies on the TASC multiplier (i_{TASC} = 1.13), labour cost indicator (i_{LC} = 0.5), engineering and project cost indicator ($i_{E\&PC}$ = 0.35), land and owner's cost ($C_{L\&O} = 198{,}940$ k€) [39], and investment costs of CaLC (C_{CaLC}), sCO2 (C_{sCO2}), and CCT (C_{CCT}).

$$C_{TASC} = i_{TASC} \cdot [(1 + i_{LC} + i_{E\&PC}) \cdot (C_{CaLC} + C_{sCO2} + C_{CCT}) + C_{L\&O}] \quad (3)$$

The investment costs of the CaLC, CCT and sCO2 cycle were estimated using the bottom-up approach, considering the capital cost of each component in the considered cases, and then the sum of costs was increased by 5% to take into account the component connection cost [48]. The correlations used for estimation of the capital cost of individual pieces of equipment in the CaLC-based power plant are presented in Table 5. The capital cost of the reference supercritical steam cycle was assumed to be 214,443 k€, based on Fout et al. [39]. The detailed description of the investment cost estimation framework is available in Michalski et al. [38].

Table 5: Estimation methodology for equipment capital cost

Equipment [scaling parameter]	Correlation
Calciner [heat flux, $\dot{Q}_{Cal}$ (kW)] [38]	$C_{Cal} = 13.14 \cdot 10^6 \cdot \dot{Q}_{Cal}^{0.67}$
Carbonator [heat flux, $\dot{Q}_{Car}$ (kW)] [38]	$C_{Car} = 16.591 \cdot 10^6 \cdot \dot{Q}_{Car}^{0.67}$
CO2 compressor [equivalent air mass flow rate, $\dot{m}_{AE,Com}$ (kg/s), isentropic efficiency, $\eta_{i,Com}$ (-), inlet pressure, p_{in} (MPa); equivalent air outlet pressure, $p_{AE,out}$ (MPa)] [49]	$C_C = \dot{m}_{AE,C} \cdot \frac{47.1}{1-\eta_{i,C}} \cdot \frac{p_{AE,out}}{p_{in}} \cdot ln\left(\frac{p_{AE,out}}{p_{in}}\right)$
CO2 expander [equivalent mass flow rate of air, $\dot{m}_{AE,C}$ (kg/s), isentropic efficiency, $\eta_{i,E}$ (-), inlet pressure, p_{in} (MPa); equivalent air outlet pressure, $p_{AE,out}$ (MPa); inlet temperature, T_{in} (K)] [50,51]	$C_E = \dot{m}_{AE,E} \cdot \frac{392.2}{1-\eta_{i,E}} \cdot \frac{p_{in}}{p_{AE,out}} \cdot ln\left(\frac{p_{in}}{p_{AE,out}}\right) \cdot$ $\cdot [1 + exp(0.036 \cdot T_{in} - 65.66)]$
CO2 pump [brake power, P_P (kW) ; isentropic efficiency, $\eta_{i,P}$ (-)] [51]	$C_P = 3531.4 \cdot P_P^{0.71}$ $\cdot \left[1 + \left(\frac{1-0.8}{1-\eta_{i,P}}\right)^3\right]$
Cooling tower [heat flux, $\dot{Q}_{Cooler}$ (kW)] [40]	$C_{CT} = 32.3 \cdot \dot{Q}_{Cooler}$
Electric generator [gross power output, P_G (kW)] [41]	$C_{EG} = 84.5 \cdot P_G^{0.95}$
Fuel preparation system [fuel flow rate, $\dot{m}_F$ (kg/s)] [38]	$C_{FP} = 14\,158\,479 \cdot \dot{m}_F^{0.24}$
Fan [break power, P_{Fan} (kW)] [41,52,53]	$C_{Fan} = 103193 \cdot \left(\frac{P_{Fan}}{445}\right)^{0.67}$
Heat exchanger [surface area, A_{HE} (m2); operating pressure, p_{HE} (bar)] [51]	$C_{HE} = 2546.9 \cdot A_{HE}^{0.67} \cdot p_{HE}^{0.28}$

3 RESULTS

3.1 Techno-economic performance under the initial design basis

The assessment of the thermodynamic performance of the considered CaLC-based power plants (Table 6) showed that among the cases with the sCO_2 cycle Case 2 had the lowest total auxiliary power requirement (70.1 MW), whereas the figure for Case 1 was the highest (72.2 MW). In contrast, the total auxiliary power requirement of the reference case was 85.4 MW, which was higher due to a higher power requirement of the supercritical steam cycle. It is also important to emphasise that CCT accounted for the major part of the total auxiliary power requirement, which accounted for 62.3–64.2% in the sCO_2 cases and 52.7% in the reference case.

An assessment of the thermal efficiency of the considered power cycles revealed (Table 6) that the recompression sCO_2 cycle (Case 2) had the highest thermal efficiency of 46.83%$_{HHV}$ among the considered cases. This figure was 0.38%$_{HHV}$ points higher than that estimated for the supercritical steam cycle (reference case). The thermal efficiencies for Case 1 and Case 3 were 6.51%$_{HHV}$ points and 1.43%$_{HHV}$ points, respectively, lower than that in Case 2. Regardless of the highest thermal efficiency, Case 2 was shown to result in the lowest net efficiency (29.89%$_{HHV}$) among the considered cases. This was because the amount of heat utilised in Case 2 is significantly lower than that in the remaining cases. Namely, the clean gas temperature at the outlet of the CaLC-based power plant was 102.8°C for Case 1 and Case 3, and 461.9°C in Case 2. Therefore, Case 2 can be deemed as not feasible from the thermodynamic standpoint and is included in the further analysis for comparison only.

The highest net power output (496.4 MW), and subsequently, the highest net efficiency (34.17%$_{HHV}$) among the sCO_2 cases were observed for Case 3. The specific CO_2 emissions in this case were estimated to be 104.4 kg/MWh. The thermodynamic performance of this case was superior to that of Case 1, for which the net efficiency was shown to be lower by 4.14%$_{HHV}$ points and specific CO_2 emission was shown to be higher by 14.4 kg/MWh. Also, the net efficiency in Case 2 was lower by 0.14% points and, subsequently, the specific CO_2 emissions were higher by 0.5 kg/MWh, compared to these in Case 1. These results showed that Case 3 is characterised with the best thermodynamic performance because it not only maximised the utilisation of heat available in CaLC, which was reflected in the low clean gas outlet temperature,

but also achieved a high thermal efficiency for the sCO_2 cycle via CO_2 recompression. Nevertheless, the net efficiency of Case 3 was still 0.93%$_{HHV}$ points lower than that of the reference case with a supercritical steam cycle. This may be explained by a higher rate of heat utilisation in the reference case, as the clean gas temperature at the outlet of the CaLC-based power plant was around 60°C [27].

Table 6: Techno-economic results under initial design basis

Parameter	Reference case	Case 1	Case 2	Case 3
Thermodynamic assessment				
Thermal power input (MW_{HHV})	1452.54	1452.54	1452.54	1452.54
CO_2 compression train power requirement (MW)	44.99	44.99	44.99	44.99
Calcium looping combustion power requirement (MW)	18.29	18.89	18.89	18.89
Supercritical steam cycle power requirement (MW)	22.14	-	-	-
Supercritical CO_2 cycle power requirement (MW)	-	8.28	6.24	7.52
Total auxiliary power requirement (MW)	85.42	72.17	70.12	71.40
Net power output (MW)	510.30	436.22	434.14	496.40
Supercritical steam cycle thermal efficiency (%$_{HHV}$)	46.45	-	-	-
Supercritical CO_2 cycle thermal efficiency (%$_{HHV}$)	-	40.32	46.83	45.40
Net efficiency (%$_{HHV}$)	35.10	30.03	29.89	34.17
Specific CO_2 emission (kg/MWh)	101.50	118.74	119.22	104.35
Economic assessment				
CO_2 compression train investment cost (M€)	23.53	23.76	23.76	23.76
Calcium looping combustion investment cost (M€)	392.26	393.54	372.33	393.54
Supercritical steam cycle investment cost (M€)	214.44	-	-	-
Supercritical CO_2 cycle investment cost (M€)	-	128.27	146.38	169.86
Total as-spent investment cost (M€)	1546.4	1368.90	1363.41	1456.07
Break-even price of electricity (€/MWh)	83.20	91.59	89.84	81.16

The economic assessment revealed that the lowest total as-spent investment cost was estimated for Case 2 (1363.41 M€) and the highest figure was estimated for Case 3 (1456.07 M€). Nevertheless, because the net efficiency in Case 3 was significantly higher than in other cases, it had the lowest BEP_{el} (81.16 €/MWh). BEP_{el} for Case 1 and Case 2 were higher by 10.43 €/MWh and 8.68 €/MWh, respectively. It needs to be noted that the total as-spent investment cost for the reference case was 6% higher (1546.4 M€) than that in Case 3. This confirms the potential for the sCO_2 cycle to reduce the capital cost and, subsequently, the footprint of the CaLC-based power plant. Yet, because of the lower net efficiency in Case 3, the BEP_{el} for the reference case was lower by 2.04 €/MWh.

3.2 Parametric study

A parametric study was conducted to identify the effect of the process parameters on

the techno-economic performance of the considered cases and to identify potential improvements. The following process parameters were considered in this analysis:

- O_2 concentration in the flue gas was varied between 1% and 3%;
- Relative sorbent make-up rate was varied between 3% and 7%;
- Turbine inlet temperature was varied between 500°C and 675°C;
- Compressor outlet pressure was varied between 18 MPa and 30 MPa;
- Temperature differences at the cold end of the HTR and the LTR, and hot end of LTR were varied between 5°C and 15°C.

It was assumed that the minimum temperature difference at the cold end of the flue gas cooler is 10°C. The results showed that this temperature difference decreases with an increase in the turbine inlet temperature and a decrease in the compressor outlet pressure. Thus, the maximum turbine inlet temperature and minimum compressor outlet pressure were constrained to 675°C and 18 MPa, respectively.

The variation in the relative sorbent make-up was shown to have the largest impact on the net efficiency in all considered cases (Figure 5). The net efficiency in Case 1 was reduced by 2.1%$_{HHV}$ points, and by 2.3%$_{HHV}$ points in both Case 2 and Case 3, on an increase of the relative sorbent make-up from 3% to 7%. Moreover, the net efficiency was less influenced on variation in the O_2 concentration in the flue gas (Figure 5). Its increase from 1% to 3% caused the net efficiency to decrease by 0.2%$_{HHV}$ points and 0.4%$_{HHV}$ points, respectively, in Case 1 and Case 3. Conversely, the net efficiency was reduced by 0.9%$_{HHV}$ points in Case 2, which is more than double that of Case 3. This was caused by a higher clean gas temperature at the outlet of the CaLC-based power plant (360°C) and, thus, higher heat loss in Case 2.

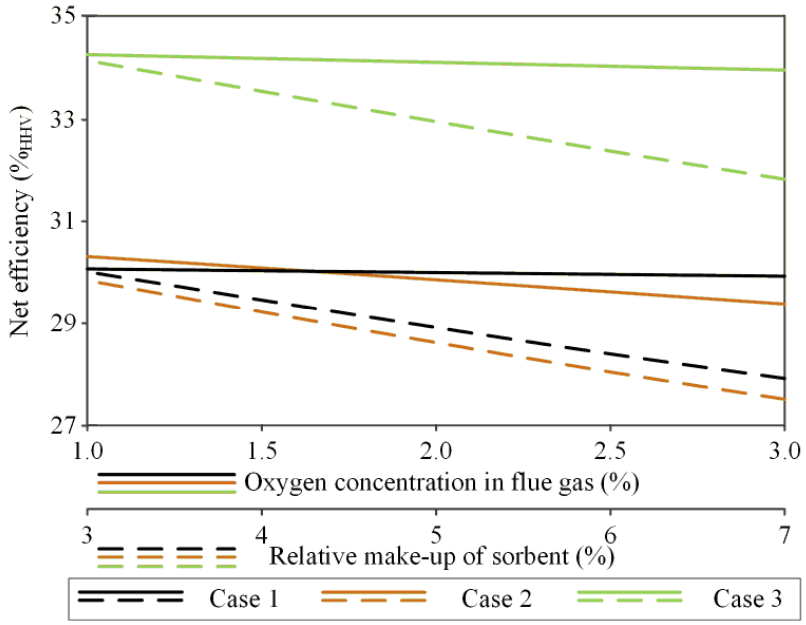

Figure 5: Effect of calcium looping combustion operating parameters on the thermodynamic performance of CaLC-based power plant

Similarly to the effect on the thermodynamic performance, the variation in the relative sorbent make-up rate was shown to have a more significant impact on the economic performance (Figure 6). An increase of the relative sorbent make-up from 3% to 7% caused an increase in BEP_{el} by 18.1 €/MWh and 19.0 €/MWh in Case 1 and Case 2, respectively. The impact was slightly lower (15.8 €/MWh) in Case 3. Importantly, the variation in the O_2 concentration in the flue gas had a negligible impact on the economic performance in all considered cases.

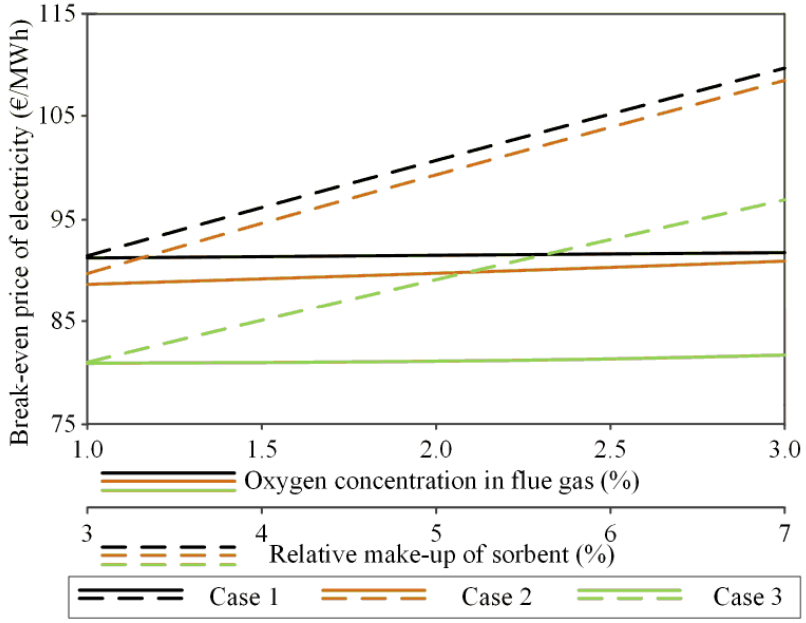

Figure 6: Effect of calcium looping combustion operating parameters on the economic performance of CaLC-based power plant

Figure 7 reveals that an optimal compressor outlet pressure was 24 MPa and 20 MPa in Case 2 and Case 3, respectively, at the turbine inlet temperature of 500°C. Similarly, an optimal compressor outlet pressure in Case 3 was 23 MPa at turbine inlet temperature of 675°C. For the remaining curves, the optimal compressor outlet pressure is above the maximum value considered in the parametric analysis. Furthermore, Figure 7 confirms that the highest net efficiency of the CaLC-based power plant is achieved at the highest turbine inlet temperature. The impact of variation in the turbine inlet temperature was shown to be higher than that of the compressor outlet pressure. Variation of the former from 500°C to 675°C caused increases in the net efficiency of 4.7%$_{HHV}$ and 7.2%$_{HHV}$ points in Case 2 and Case 3, respectively, whereas variation in the latter led to increases in the net efficiency by 0.3–2.6%$_{HHV}$ points.

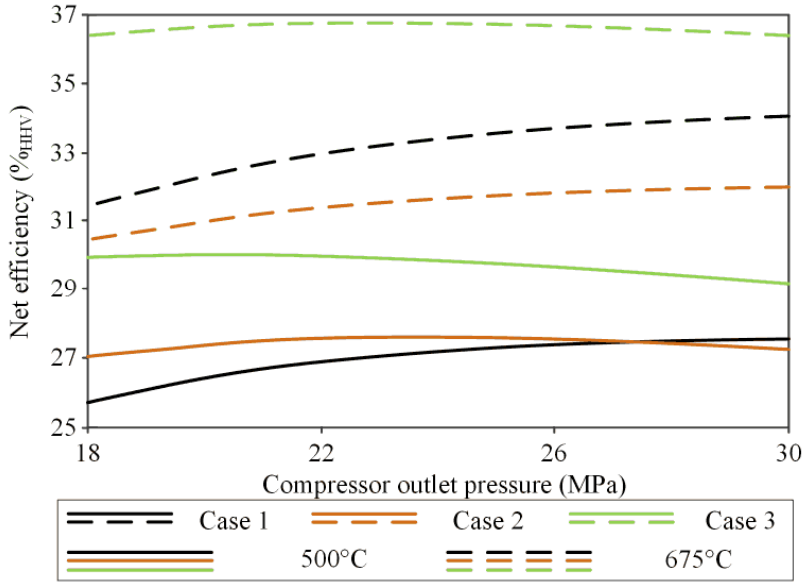

Figure 7: Effect of CO_2 temperature at the inlet to the expander and the main compressor outlet pressure on the thermodynamic performance of calcium looping combustion-based power plant

Figure 8 indicates that the BEP_{el} decreased with an increase in the turbine inlet temperature, along with increased net efficiency. At 675°C, the optimal main compressor outlet pressures of 27 MPa and 21 MPa were observed in Case 2 and Case 3, respectively. In Case 1, the change in BEP_{el} at the compressor outlet pressure

between 27–30 MPa was shown to be negligible.

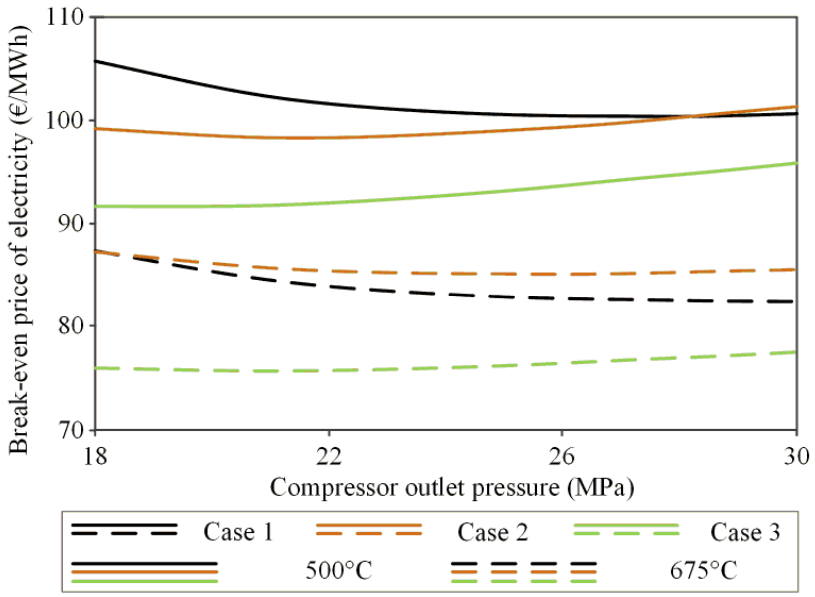

Figure 8: Effect of CO_2 temperature at the inlet to the expander and the main compressor outlet pressure on the economic performance of calcium looping combustion-based power plant

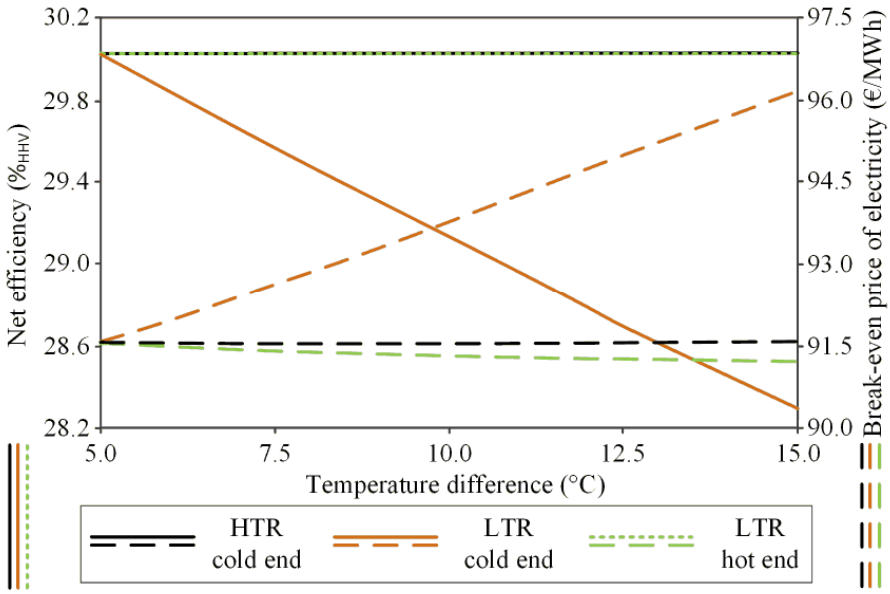

Figure 9: Effect of the temperature differences of the heat exchangers on the techno-economic performance in Case 1

Figure 9 revealed that the techno-economic performance in Case 1 is marginally influenced by the change in the temperature difference at the hot end of the LTR and the cold end of the HTR. This is because a negligible impact on the net efficiency and marginal impact on the BEP_{el} were observed. Finally, the temperature difference at the cold end of the LTR had a significant impact on the techno-economic performance in Case 1. This can be associated with a 1.7%$_{HHV}$-points decrease in the net efficiency

on the increase in the temperature difference from 5°C to 15°C. Importantly, the increased temperature difference at the cold end of the LTR resulted in more heat removed in the cooler. In turn, less heat was available for power generation, leading to a decrease in the gross power output. In this vein, the BEP_{el} decreased by 4.62 €/MWh on an increase of the temperature difference from 5°C to 15°C. This is because the decrease in the capital cost of the LTR, which can be associated with reduced heat transfer rate, was lower than a corresponding increase in the capital costs of the cooler and cooling tower.

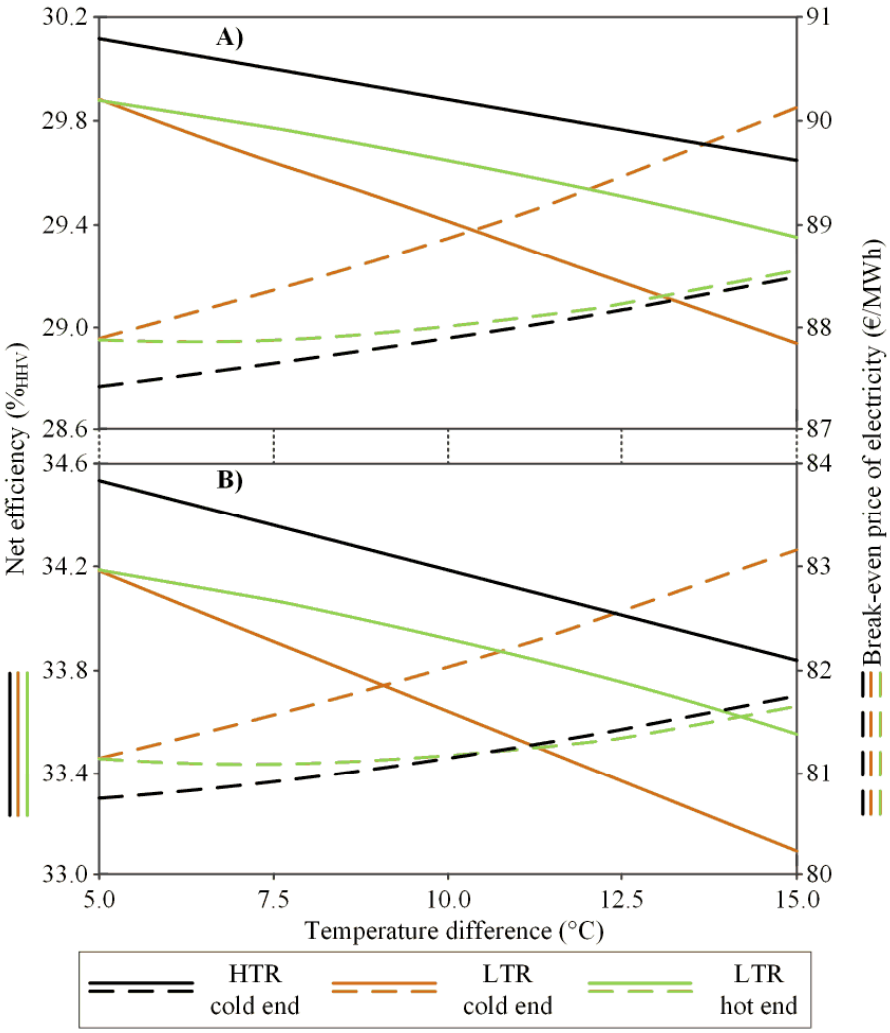

Figure 10: Effect of the temperature differences of the heat exchangers on the techno-economic performance in supercritical CO_2 cycle A) Case 2 and B) Case 3

The results of the parametric study for Case 2 and Case 3 presented in Figure 10 revealed that, in both cases, the change of temperature difference at the cold end of the HTR from 5°C to 15°C had a significantly larger impact on the thermodynamic and economic indicators than in Case 1. Namely, the net efficiency decreased by 0.5%HHV and 0.7%HHV points in Case 2 and Case 3, respectively, and the BEP_{el} increased by 1

€/MWh in both cases. Variation of the temperature difference at the hot end of the LTR resulted in similar results, as the net efficiency decreased by 0.5–0.6%$_{HHV}$ points and the BEP_{el} increased by 0.55–0.64 €/MWh. As in Case 1, the increase in the temperature difference at the cold end of the LTR had the largest impact on the techno-economic performance. The net efficiency decreased by 0.9%$_{HHV}$ and 1.1%$_{HHV}$ points, whereas the BEP_{el} increased by 2.23 €/MWh and 2.01 €/MWh in Case 2 and Case 3, respectively.

4 DISCUSSION

The techno-economic performance of the considered cases was assessed under the revised design basis, incorporating results from the parametric study. In all cases, the O_2 concentration in flue gas of 1% and the turbine inlet temperature of 675°C were assumed. Remaining revised parameters, along with the thermodynamic and economic results are presented in Table 7. Under the revised design basis, a significant improvement in the techno-economic performance was observed, as the net efficiency increased by 4.2%$_{HHV}$ points, 2.6%$_{HHV}$ points, and 3.1%$_{HHV}$ points and the BEP_{el} reduced by 9.42 €/MWh, 5.91 €/MWh and 6.03 €/MWh in Case 1, Case 2 and Case 3, respectively.

Table 7: Techno-economic results under revised design basis

Parameter	Reference case	Case 1	Case 2	Case 3
Assumptions				
Main compressor outlet pressure (MPa)	-	30.0	27.0	21.0
High-temperature recuperator cold-end temperature difference (°C)	-	7.5	5.0	5.0
Thermodynamic assessment				
Thermal power input (MW_{HHV})	1452.54	1452.54	1452.54	1452.54
Supercritical steam cycle thermal efficiency (%$_{HHV}$)	46.45	-	-	-
Supercritical CO_2 cycle thermal efficiency (%$_{HHV}$)	-	45.33	50.47	49.16
CO_2 compression train power requirement (MW)	44.99	44.97	44.99	44.98
Calcium looping combustion power requirement (MW)	18.29	18.29	18.29	18.29
Supercritical CO_2 cycle power requirement (MW)	22.14	7.49	5.76	7.01
Total auxiliary power requirement (MW)	85.42	70.75	69.04	70.29
Net power output (MW)	510.3	496.59	472.22	541.83
Net efficiency (%$_{HHV}$)	35.10	34.19	32.51	37.30
Specific CO_2 emission (kg/MWh)	101.50	104.32	109.69	95.55
Economic assessment				
CO_2 compression train investment cost (M€)	23.53	23.75	23.76	23.75
Calcium looping combustion investment cost (M€)	392.26	392.57	372.33	392.88
Supercritical steam cycle investment cost (M€)	214.44	-	-	-
Supercritical CO_2 cycle investment cost (M€)	-	157.43	168.35	184.47
Total as-spent investment cost (M€)	1546.4	1427.95	1408.45	1485.27
Break-even price of electricity (€/MWh)	83.20	82.17	83.94	75.13

Compared to the reference case, the net efficiency of Case 3 under the revised design

basis is 2.2%$_{HHV}$ points higher (Table 7). Such a net efficiency is only 0.7%$_{HHV}$ points lower than that of a conventional coal-fired power plant without CO_2 capture (38%$_{HHV}$) [38]. Furthermore, the BEP_{el} in Case 3 is 8.07 €/MWh lower than that in the reference case. Yet, compared to the conventional coal-fired power plant (59.63 €/MWh) [38], CaLC-based power plant with the recompression sCO_2 cycle and the CGC (Case 3) will still result in a 26% increase in the BEP_{el}. Nevertheless, such results confirm the potential of the advanced power cycles to improve the techno-economic performance of CaLC-based power plants.

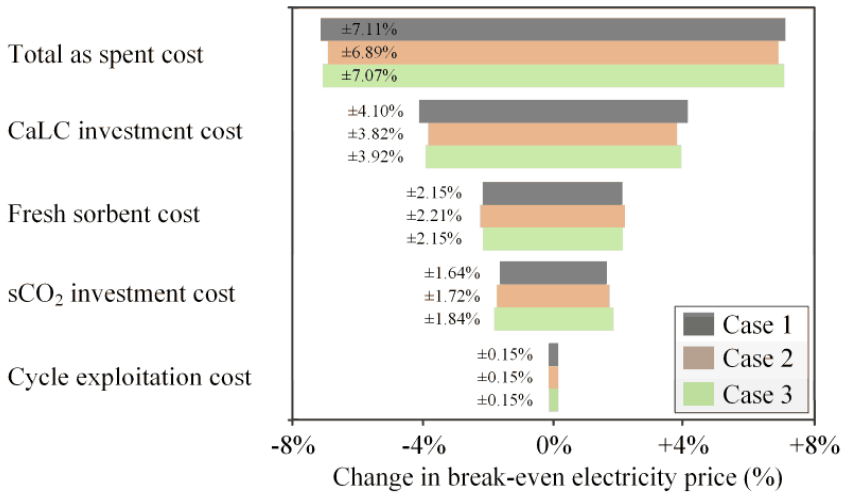

Figure 11. Economic sensitivity analysis results of CaLC-based power plant

Because of the uncertainty in the economic data associated with the emerging technologies, such as CaLC, a sensitivity analysis of the key economic parameters was performed. This was achieved by varying the value of the selected parameters by ±15%, based on the assumptions presented in Table 4, and assessing their impact on the estimation of BEP_{el}. The results presented in Figure 11 revealed that BEP_{el} changed by ±6.9–7.1% on a ±15 variation in the TASC, which is less than half the simulated change in the TASC value. The influence of the CaLC and sCO_2 investment cost was even lower, as a ±15 variation in these parameters resulted in ±3.92–4.1% and ±2.15–2.21% change in BEP_{el}, respectively. Finally, the results showed that the change of the sorbent cost has a higher influence on economic performance than sCO_2 investment cost and that the influence of the cycle exploitation cost is negligible. Overall, the uncertainty in the economic data has a small influence on the accuracy of BEP_{el} estimation.

5 CONCLUSIONS

This study proposed three strategies to integrate the sCO_2 cycle with CaLC and evaluated their techno-economic performance at different operating conditions to maximise the techno-economic feasibility of the CaLC-based power plant. The economic performance was evaluated using the NPV approach. The results showed that to achieve the best techno-economic performance, the structure of the sCO_2 cycle needs to both maximise heat utilisation from CaLC and the cycle thermal efficiency. The CaLC-based power plant with the recompression sCO_2 cycle and the CGC (Case 3) was shown to have the best performance among all considered cases. Having revised the operating conditions of the sCO_2 cycle through parametric studies, this case achieved a net efficiency and a BEP_{el} of 37.3%$_{HHV}$ and 75.13 €/MWh, respectively. Such a net efficiency is only 0.7%$_{HHV}$ point lower, and the BEP_{el} is 26% higher than that of a conventional coal-fired power plant without CO_2 capture. Further work should consider the application of advanced sorbents and assess the uncertainty effect on the prediction of the economic performance of the CaLC-based coal-fired power plant.

Acknowledgements

This publication is based on research conducted within the “Redefining power generation from carbonaceous fuels with carbonate looping combustion and gasification technologies” project funded by UK Engineering and Physical Sciences Research Council (EPSRC reference: EP/P034594/1).

References

[1] The Intergovernmental Panel on Climate Change. Global Warming of 1.5 ºC 2018.

[2] International Energy Agency. Key world energy statistics. Paris, France: IEA Publications; 2018.

[3] International Energy Agency. Global Energy & CO_2 Status Report 2019.

[4] International Energy Agency. Coal 2018. Analysis and Forecasts to 2023. Paris, France: IEA Publications; 2018.

[5] IEA. Tracking Clean Energy Progress 2013. IEA Input to the Clean Energy Ministerial. Paris, France: IEA Publications; 2013.

[6] Miller BG. Clean Coal Engineering Technology 2011.

[7] IEA. Climate Change and Enviroment 2016 Insights. Paris, France: IEA Publications; 2016.

[8] Van Vuuren DP, Stehfest E, Gernaat DEHJ, Van Den Berg M, Bijl DL, De Boer HS, Daioglou V, Doelman JC, Edelenbosch OY, Harmsen M, Hof AF, van Sluisveld MAE. Alternative pathways to the 1.5 °C target reduce the need for negative emission technologies. Nat Clim Chang 2018;8:391–7. doi:10.1038/s41558-018-0119-8.

[9] Bui M, Adjiman CS, Bardow A, Anthony EJ, Boston A, Brown S, Fennell PS, Fuss S, Galindo A, Hackett LA, Hallett JP, Herzog HJ, Jackson G, Kemper J, Krevor S, Maitland GC, Matuszewski M, Metcalfe IS, Petit C, Puxty G, Reimer J, Reiner DM, Rubin ES, Scot SA, Shah N, Smit B, Trusler JPM, Webley P, Wilcox J, Mac Dowell N. Carbon capture and storage (CCS): the way forward. Energy Environ Sci 2018;11:1062–176. doi:10.1039/C7EE02342A.

[10] Mantripragada HC, Zhai H, Rubin ES. Boundary Dam or Petra Nova – Which is a better model for CCS energy supply? Int J Greenh Gas Control 2019;82:59–68. doi:10.1016/j.ijggc.2019.01.004.

[11] Oko E, Ramshaw C, Wang M. Study of intercooling for rotating packed bed absorbers in intensified solvent-based CO_2 capture process. Appl Energy 2018;223:302–16. doi:10.1016/j.apenergy.2018.04.057.

[12] Zhang S, Chen C, Ahn WS. Recent progress on CO_2 capture using amine-functionalized silica. Curr Opin Green Sustain Chem 2019;16:26–32. doi:10.1016/j.cogsc.2018.11.011.

[13] Borhani TN, Wang M. Role of solvents in CO_2 capture processes: the review of selection and design methods. Renew Sustain Energy Rev 2019;114:109299. doi:10.1016/j.rser.2019.109299.

[14] Abanades JC, Anthony EJ, Wang J, Oakey JE. Fluidized bed combustion systems integrating CO_2 capture with CaO. Environ Sci Technol 2005;39:2861–2866. doi:10.1021/es0496221.

[15] Arias B, Diego ME, Abanades JC, Lorenzo M, Diaz L, Martínez D, Alvarez J, Sánchez-Biezma A. Demonstration of steady state CO_2 capture in a 1.7MW_{th} calcium looping pilot. Int J Greenh Gas Control 2013;18:237–45. doi:10.1016/j.ijggc.2013.07.014.

[16] Chang M-H, Chen W-C, Huang C-M, Liu W-H, Chou Y-C, Chang W-C, Chen W, Cheng J-Y, Huang K-E, Hsu H-W. Design and experimental testing of a 1.9MW_{th} calcium looping pilot plant. Energy Procedia 2014;63:2100–8. doi: 10.1016/j.egypro.2014.11.226.

[17] Hanak DP, Anthony EJ, Manovic V. A review of developments in pilot plant testing and modelling of calcium looping process for CO_2 capture from power generation systems. Energy Environ Sci 2015;8:2199–2249. doi:10.1039/C5EE01228G.

[18] Berstad D, Anantharaman R, Blom R, Jordal K, Arstad B. NGCC post-combustion CO_2 capture with Ca/carbonate looping: Efficiency dependency on sorbent properties, capture unit performance and process configuration. Int J Greenh Gas Control 2014;24:43–53. doi:10.1016/j.ijggc.2014.02.015.

[19] Rodríguez N, Alonso M, Abanades JC. Average activity of CaO particles in a calcium looping system. Chem Eng J 2010;156:388–94. doi:http://dx.doi.org/10.1016/j.cej.2009.10.055.

[20] Cormos C-C. Economic evaluations of coal-based combustion and gasification power plants with post-combustion CO_2 capture using calcium looping cycle. Energy 2014;78:665–73. doi:10.1016/j.energy.2014.10.054.

[21] Hanak DP, Biliyok C, Anthony EJ, Manovic V. Modelling and comparison of calcium looping and chemical solvent scrubbing retrofits for CO_2 capture from coal-fired power plant. Int J Greenh Gas Control 2015;42:226–36. doi:10.1016/j.ijggc.2015.08.003.

[22] Hanak DP, Erans M, Nabavi SA, Jeremias M, Romeo LM, Manovic V. Technical and economic feasibility evaluation of calcium looping with no CO_2 recirculation. Chem Eng J 2018;335:763–73. doi:10.1016/J.CEJ.2017.11.022.

[23] Erans M, Hanak DP, Mir J, Anthony EJ, Manovic V. Process modelling and techno-economic analysis of natural gas combined cycle integrated with calcium looping. Therm Sci 2016;20:59–67. doi:10.2298/TSCI151001209E.

[24] Rolfe A, Huang Y, Haaf M, Rezvani S, Dave A, Hewitt NJ. Techno-economic and environmental analysis of calcium carbonate looping for CO_2 capture from a pulverised coal-fired power plant. Energy Procedia 2017;142:3447–53. doi:10.1016/j.egypro.2017.12.228.

[25] Rolfe A, Huang Y, Haaf M, Rezvani S, McIlveen-Wright D, Hewitt NJ. Integration of the calcium carbonate looping process into an existing pulverized coal-fired power plant for CO_2 capture: Techno-economic and environmental evaluation. Appl Energy 2018;222:169–79. doi:10.1016/j.apenergy.2018.03.160.

[26] Williams BC, Mcmullan JT. Techno-economic analysis of fuel conversion and power generation systems - The development of a portable chemical process simulator with capital cost and economic performance analysis capabilities. Int J Energy Res 1996;20:125–42. doi:10.1002/(SICI)1099-114X(199602)20:2<125::AID-ER239>3.0.CO;2-2.

[27] Hanak DP, Manovic V. Calcium looping combustion for high-efficiency low-emission power generation. J Clean Prod 2017;161:245–55. doi:10.1016/j.jclepro.2017.05.080.

[28] Marchionni M, Bianchi G, Tsamos KM, Tassou SA. Techno-economic

comparison of different cycle architectures for high temperature waste heat to power conversion systems using CO_2 in supercritical phase. Energy Procedia 2017;123:305–12. doi:10.1016/j.egypro.2017.07.253.

[29] Garcia RF. Efficiency enhancement of combined cycles by suitable working fluids and operating conditions. Appl Therm Eng 2012;42:25–33. doi:10.1016/j.applthermaleng.2012.02.039.

[30] Kunitomi K, Katanishi S, Takada S, Takizuka T, Yan X. Japan's future HTR - The GTHTR300. Nucl Eng Des 2004;233:309–27. doi:10.1016/j.nucengdes.2004.08.026.

[31] Feher EG. The supercritical thermodynamic power cycle. Energy Convers 1968;8:85–90. doi:10.1016/0013-7480(68)90105-8.

[32] Michalski S, Hanak DP, Manovic V. Advanced power cycles for coal-fired power plants based on calcium looping combustion: A techno-economic feasibility assessment. Appl Energy 2020;269:114954. doi:10.1016/j.apenergy.2020.114954.

[33] Dostal V, Driscoll MJ., Hejzlar P. A supercritical carbon dioxide cycle for next generation nuclear reactors. Cambridge, MA, USA: Massachusetts Institute of Technology; 2004.

[34] Le Moullec Y. Conceptual study of a high efficiency coal-fired power plant with CO_2 capture using a supercritical CO_2 Brayton cycle. Energy 2013;49:32–46. doi:10.1016/j.energy.2012.10.022.

[35] Hanak DP, Manovic V. Calcium looping with supercritical CO_2 cycle for decarbonisation of coal-fired power plant. Energy 2016;102. doi:10.1016/j.energy.2016.02.079.

[36] Wei X, Manovic V, Hanak DP. Techno-economic assessment of coal- or biomass-fired oxy-combustion power plants with supercritical carbon dioxide cycle. Energy Convers Manag 2020;221:113143. doi:10.1016/j.enconman.2020.113143.

[37] Sánchez-Biezma A, Paniagua J, Diaz L, Lorenzo M, Alvarez J, Martínez D, Arias B, Diego ME, Abanades JC. Testing postcombustion CO_2 capture with CaO in a 1.7 MW_t pilot facility. Energy Procedia 2013;37:1–8. doi:http://dx.doi.org/10.1016/j.egypro.2013.05.078.

[38] Michalski S, Hanak DP, Manovic V. Techno-economic feasibility assessment of calcium looping combustion using commercial technology appraisal tools. J Clean Prod 2019;219:540–51. doi:10.1016/j.jclepro.2019.02.049.

[39] Fout T, Zoelle A, Keairns D, Turner M, Woods M, Kuehn N, Shah V, Chou V, Pinkerton L. Cost and performance baseline for fossil energy plants volume 1a: bituminous coal (PC) and natural gas to electricity. Pittsburgh, PA, USA: National Energy Technology Laboratory; 2015.

[40] Park JH, Bae SW, Park HS, Cha JE, Kim MH. Transient analysis and validation with experimental data of supercritical CO_2 integral experiment loop by using MARS. Energy 2018;147:1030–43. doi:10.1016/j.energy.2017.12.092.

[41] Hanak DP, Manovic V. Combined heat and power generation with lime production for direct air capture. Energy Convers Manag 2018;160:455–66. doi:

10.1016/j.enconman.2018.01.037

[42] Ma L-C, Castro-Dominguez B, Kazantzis NK, Ma YH. Economic performance evaluation of process system design flexibility options under uncertainty: the case of hydrogen production plants with integrated membrane technology and CO_2 capture. Comput Chem Eng 2017;99:214–229. doi: 10.1016/j.compchemeng.2017.01.020.

[43] Ma L-C, Castro-Dominguez B, Kazantzis NK, Ma YH. Integration of membrane technology into hydrogen production plants with CO_2 capture: An economic performance assessment study. Int J Greenh Gas Control 2015;42:424–38. doi:10.1016/j.ijggc.2015.08.019.

[44] Steinbach J, Staniaszek D. Discount rates in energy system analysis – Discussion Paper. Buildings Performance Institue Europe (BPIE); 2015.

[45] Eurostat. Database - Eurostat 2018. http://ec.europa.eu/eurostat/data/database (accessed May 21, 2018)

[46] EDF Energy. Cottam and West Burtony 2018. https://www.edfenergy.com/energy/power-stations/cottam-west-burton-a (accessed May 21, 2018)

[47] EURACOAL. Market report 2/2017. EURACOAL; 2017.

[48] Peters MS, Timmerhaus KD, West RE. Plant Design and Economics for Chemical Engineers. 5th ed. New York, NY, USA: McGraw-Hill; 2003.

[49] Benjelloun M, Doulgeris G, Singh R. A method for techno-economic analysis of supercritical carbon dioxide cycles for new generation nuclear power plants. Proc Inst Mech Eng Part A J Power Energy 2012;226:372–83. doi:10.1177/0957650911429643.

[50] Criado YA, Arias B, Abanades JC. Calcium looping CO_2 capture system for back-up power plants. Energy Environ Sci 2017;10:1994–2004. doi:10.1039/C7EE01505D.

[51] Gabbrielli R, Singh R. Economic and scenario analyses of new gas turbine combined cycles with no emissions of carbon dioxide. J Eng Gas Turbines Power 2005;127:531. doi:10.1115/1.1850492.

[52] Shirazi A, Aminyavari M, Najafi B, Rinaldi F, Razaghi M. Thermal-economic-environmental analysis and multi-objective optimization of an internal-reforming solid oxide fuel cell-gas turbine hybrid system. Int J Hydrogen Energy 2012;37:19111–24. doi:10.1016/j.ijhydene.2012.09.143.

[53] Lee YD, Ahn KY, Morosuk T, Tsatsaronis G. Exergetic and exergoeconomic evaluation of a solid-oxide fuel-cell-based combined heat and power generation system. Energy Convers Manag 2014;85:154–64. doi:10.1016/j.enconman.2014.05.066.

List of abbreviations

BEP_{el}	Break-even electricity price
CaL	Carbonate looping
CaLC	Carbonate looping combustion
CBC	Closed Brayton cycle
CCS	Carbon capture and storage
CCT	CO_2 compression train
CFPP	Coal-fired power plant
CGC	Clean gas cooler
CO_2-C	CO_2 compressor
CO_2-E	CO_2 expander
CON	CO_2 condenser
GHG	Greenhouse gas
HHV	Higher heating value
HTR	High-temperature recuperator
LTR	Low-temperature recuperator
NGCC	Natural gas combined cycle
NPV	Net present value
REC	CO_2 recompressor
sCO_2	Supercritical CO_2 cycle
TASC	Total as-spent investment cost
TRL	Technology readiness level

Nomenclature

$\dot{m}_F$	Fuel flow rate (kg/s)
C_{CCT}	Investment costs of CO_2 compression train (€)
C_{CaLC}	Investment costs of calcium looping combustion (€)
CF	Annual cash flow (€)
C_{TASC}	Total as-spent investment cost (€)
$C_{L\&O}$	Land and owner's cost (€)
C_{sCO2}	Investment costs of supercritical CO_2 cycle (€)
P_G	Gross power output (MW)
$i_{E\&PC}$	Engineering and project cost indicator (-)
i_{LC}	Labour cost indicator (-)
i_{TASC}	Total as-spent cost multiplier (-)
HHV	Higher heating value (MJ/kg)
NPV	Net present value (€)
r	Discount rate (%)
$\sum P_{AUX}$	Total auxiliary power requirement (MW)
η_N	Net efficiency (%HHV)